Embedded System Design for Reliable Portable Health Diagnostics

by

Christopher D. Lue Sang

A Thesis Presented in Partial Fulfillment
of the Requirements for the Degree
Master of Science

Approved November 2022 by the
Graduate Supervisory Committee:

Jennifer M. Blain Christen, Chair
Sule Ozev
Michael Goryll
Gregory Raupp

ARIZONA STATE UNIVERSITY

December 2022

ABSTRACT

Portable health diagnostic systems seek to perform medical grade diagnostics in non-ideal environments. This work details a robust fault tolerant portable health diagnostic design implemented in hardware, firmware and software for the detection of HPV in low-income countries. The device under device under test (DUT) is a fluorescence based lateral flow assay (LFA) point-of-care (POC) device.

This work's contributions are: firmware and software development, calibration routine implementation, device performance characterization and a proposed method of in-software fault detection. Firmware was refactored from the original implementation of the POC fluorescence reader to expose an application programming interface (API) via USB. Companion software available for desktop environments (Windows, Mac and Linux) was created to interface with this firmware API and conduct macro level routines to request and receive fluorescence data while presenting a user-friendly interface to clinical technicians.

Lastly, an environmental chamber was constructed to conduct sequential diagnostic reads in order to observe sensor drift and other deviations that might present themselves in real-world usage. The results from these evaluations show a standard deviation of less than 1% in fluorescence readings in nominal temperature environments (approx. 25°C) suggesting that this system will have a favorable signal-to-noise (SNR) ratio in such a setting. In non-ideal over heated environments ($\geq$38°C), the evaluation results showed performance degradation with standard deviations as large as 15%.

ACKNOWLEDGMENTS

This work would not have been possible without the support and mentorship of Dr. Jennifer Blain Christen. Her tireless effort and deep expertise enabled this research. Her former PhD student, Dr. Uwadiae Obahiagbon, created the initial POC prototypes. I met with Dr. Blain Christen and Dr. Obahiagbon in the Fall of 2018 as an undergraduate student. My background in software development and experience with the Arduino platform allowed me to make the first set of improvements to the POC reader firmware and desktop application.

I would also like to thank Dr. Gregory Raupp, Anthony Bajoras and Jake Snyder at MedTech Ventures (MTV). I was lucky enough to be a program assistant for MTV during my graduate work. The skills, network and perspective provided by that program played an instrumental role in my dedication and approach to this work.

Additionally, I would like to thank everyone involved in the BioElectrical Systems & Technology Lab (BEST Lab) - Joshua Eger, Ian Akamine, Vi Nguyn, Michael Hansen, Sai Prasanna Kumar Vadnala, Jonathan Garich, Nick Fritz and many more. Their camaraderie and expertise helped me fill in the gaps countless times throughout this and other projects.

I am also very thankful for Dr. Karen S. Anderson, and her team, who developed the LFAs and other biochemical products/processes needed for this system. Similarly, the hard work of our collaborators at the All India Institute of Medical Sciences (AIIMS) must be acknowledged. Many late nights (or early mornings depending on your timezone) were spent troubleshooting and debugging this system remotely. In particular, a special thanks to Dr. Pankaj Kumar - and his patience - is needed for being my troubleshooting counterpart halfway around the world.

TABLE OF CONTENTS

CHAPTER Page

LIST OF FIGURES

Figure Page

Figure Page

Figure Page

Chapter 1

INTRODUCTION

1.1 Human Papillomavirus (HPV) Prevalence

HPV is one of the leading causes of cervical cancer globally. The majority of HPV infections, between 70 - 90%, are asymptomatic and do not necessarily lead to cancer. In fact, out of over 200 different genotypes of HPV, only 12 types are classified as carcinogenic to humans. And out of those 12, HPV16 and HPV18, are responsible for 70% of cervical cancer cases, Serrano *et al.* (2018).

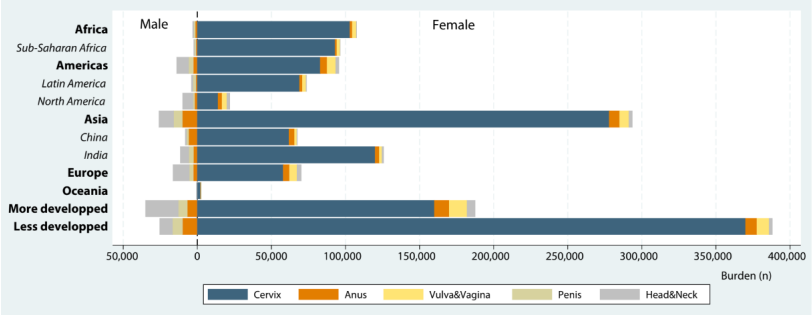

Figure 1.1: Burden of HPV-related Cancer Cases Attributable to HPV Infection by Cancer Site and HPV Vaccine from "Epidemiology and Burden of HPV-related Disease" by Serrano *et al.* (2018).

The ability to narrow down the possible causes of one of the most deadly and debilitating diseases one can contract, presents a wonderful opportunity to have an asymmetrical reward for the amount of effort required to identify biomarkers related to HPV16 and HPV18. We know that routine medical exams to track and monitor HPV; as well as, access to HPV vaccines decrease the prevalence of HPV. In developed

parts of the world where this medical infrastructure is available, we see a significant reduction in HPV prevalence (see Figure 1.2, 1.1).

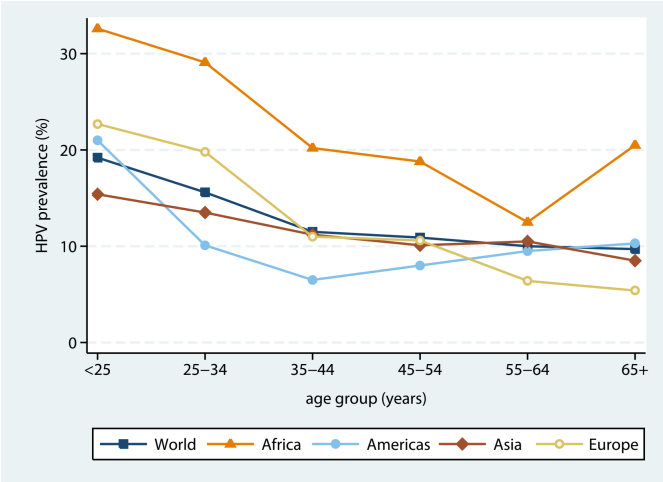

Figure 1.2: Crude Age-specific HPV Prevalence (%) in Women with Normal Cervical Cytology in the World and Its Regions. From "Epidemiology and Burden Of HPV-related Disease" by Serrano *et al.* (2018).

1.2 Point-of-Care Devices

The standard diagnostic technique for most viral infections is to send patient samples to a centralized laboratory (Naseri *et al.* (2022)). The techniques and equipment used at these facilities are costly. More aptly these facilities rely on having a developed clinical infrastructure that enable this level of care: laboratories, trained personnel and sophisticated testing equipment.

In response to these limitations, point-of-care (POC) diagnostics have been developed to serve a broader market. Moreover, the WHO has defined a class of POC diagnostics under the ASSURED criteria. ASSURED stands for: Affordable, Sensitive, Specific, User-friendly, Rapid and Robust, Equipment-free and Deliverable. There are many challenges in developing an ASSURED POC device. Primarily, cost

is the limiting factor. Expensive materials and processes must give way to cheaper alternatives and the resulting compromises in sensitivity and specificity must be rebuffed through clever engineering and dedicated research.

1.3 Lateral Flow Assays

One of the most cost effective and popular methods of detecting infection diseases incorporate lateral flow assays (LFAs). LFAs are composed of four main components: a sample pad, a conjugate pad, a reaction membrane (containing the detection line and control line) and an absorbent pad, Sohrabi *et al.* (2022) (see Figure 1.3).

LFAs can be multiplexed - meaning they contain multiple detection lines - so that they can detect multiple biomarkers within a patient sample.

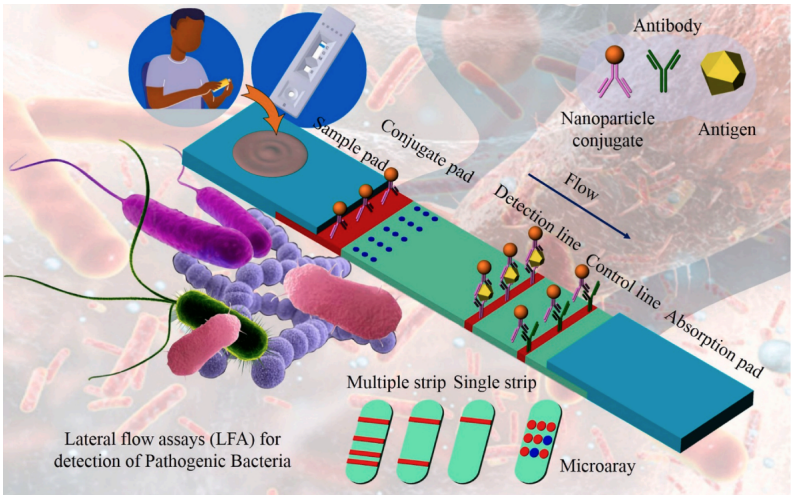

Figure 1.3: Lateral Flow Assay Design for Detecting Pathogenic Bacteria by Sohrabi *et al.* (2022)

1.4 Low-Cost HPV16 POC Diagnostic Platform

In the case of HPV16, LFAs can be utilized to detect antibodies that arise as a result of the presence of HPV. The presence of these antibodies occur in low concen-

trations. This makes detecting them difficult so special instrumentation is needed to read the detection lines present in LFAs designed for this purpose.

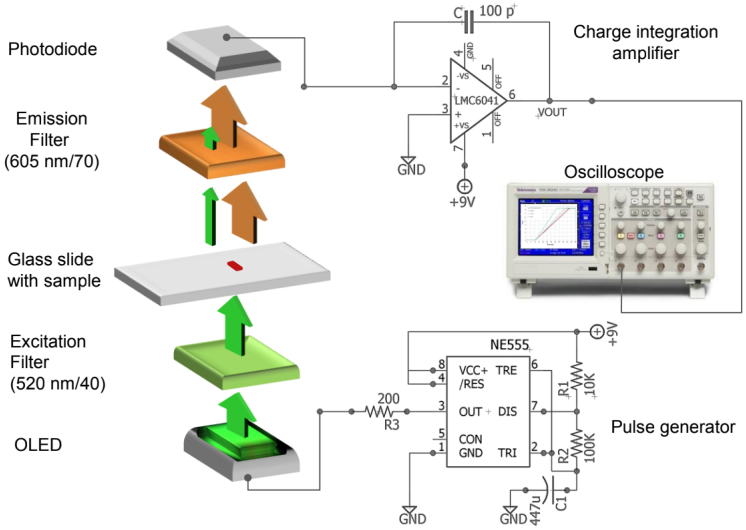

Figure 1.4: Single Site Test-Bench Fluorescence Detector by Obahiagbon (2018)

One promising design relies on a fluorescing biomarker that binds to the analyte of a detection line. This system was developed in stages. Initially utilizing a lab-bench setup with an organic light emitting diode (OLED) as the excitation source and a photodiode/charge capacitor pair for detecting the fluorescing light (see Figure 1.4).

In controlled environments, with known levels of diluted fluorescing beads, this system was refined into a multi-site fluorescence detector (see Figure 1.5). The operating principle correlates a solution concentration of an analyte with a charge integration time over a capacitor. As the sample under detection fluoresces, the charge over the capacitor builds. The higher the fluorescence the quicker the voltage 'ramps' up to the supply voltage level. In other words, higher concentration leads to faster integration time (or steeper integration slopes)

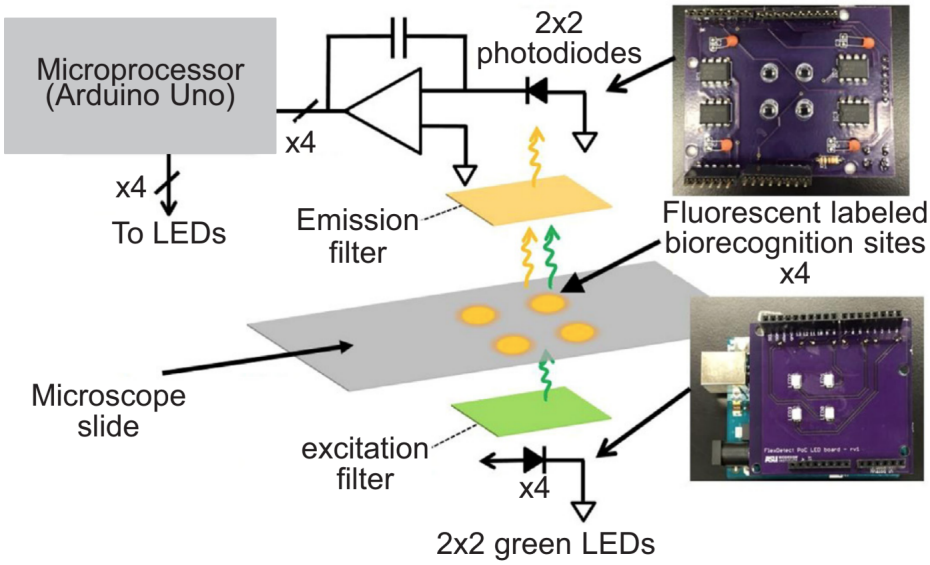

Figure 1.5: 2x2 Fluorescence Detection Platform by Obahiagbon *et al.* (2018)

1.5 Implementation Goals

The ultimate goal of this detection platform is to develop a POC system that is available in low resource settings. The original work by Obahiagbon et al. sought to incorporate this system into a user friendly platform that made generating the data simple and extracting the results of the fluorescent readings painless. Figure 1.6 depicts a high level block diagram of such a system.

1.6 Specific Aims

This work seeks to realize this vision. Specifically this work presents: an embedded system for an eight site (4x4) fluorescence detection platform. Furthermore, this work presents a companion software application that incorporates reliable communication over USB serial and which conducts regression analysis on fluorescence data that can be used to increase the reliability of diagnostic results.

lastly, the firmware and software developed for this research is to be used on

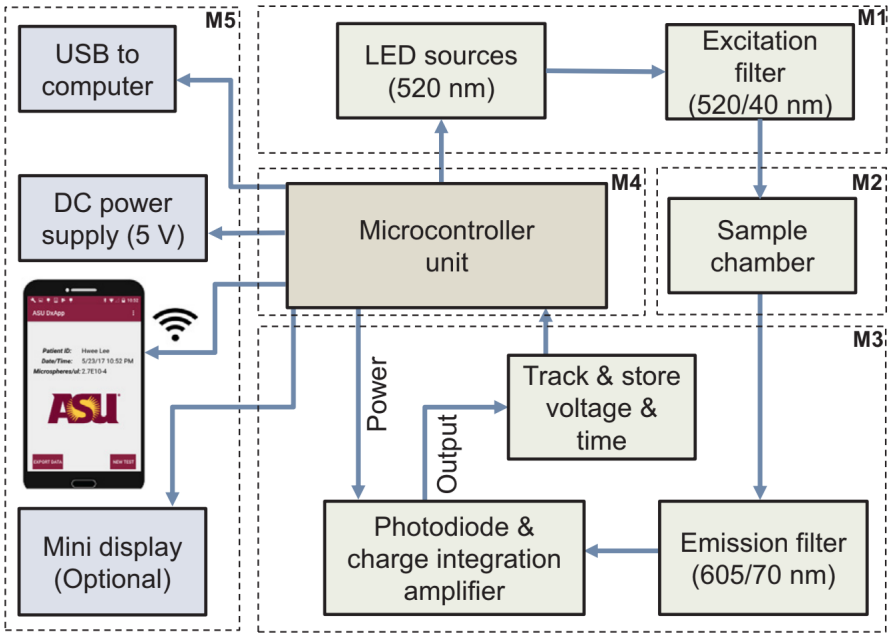

Figure 1.6: Functional Block Diagram of Proposed POC Platform Utilizing Low-Cost OTS Components by Obahiagbon *et al.* (2018)

real world patient data for the detection of HPV with collaborators at the All India Institute of Medical Sciences (AIIMS) and Baylor University. The deployment of this platform to multiple collaborators in various environments requires a flexible system that can account for variations in environments and that can inform the user of faulty hardware. To accomplish this, a calibration routine is incorporated into the POC software as well as live diagnostic readings and manual control of diagnostic emission levels (as needed).

The research presented here details: the implementation details of the hardware, the implementation details of the software and the results of the evaluation trails performed to verify the POC reader's functionality. The scope of the work presented in this paper does not include real patient samples, but does support future work of that nature.

Chapter 2

SYSTEM LEVEL DESIGN, ARCHITECTURE & APPLICATION

The point-of-care system is designed to be used in conjunction with a personal computer (see Figure 2.1). Along with the reader hardware, a companion desktop application is available for MacOS, Windows and Linux. The desktop application communicates with the POC hardware while guiding the user through various required steps.

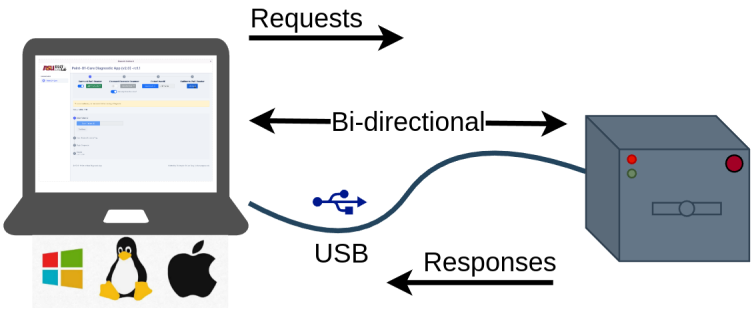

Figure 2.1: PC and Point-of-Care Reader Communication

Specifically, the desktop application allows the user to: 1) connect to a POC reader, 2) connect a barcode scanner, 3) calibrate the POC reader and 4) run a diagnostic on a patient sample.

Communication between the desktop application and the POC reader is done via javascript object notation (JSON) messages. JSON allows for key-value pair transmission in a relatively flexible manner. Requests are sent under the 'req' key. And if applicable, requests are also sent with a key called 'params' whose value reflects the parameters necessary to process the desired request.

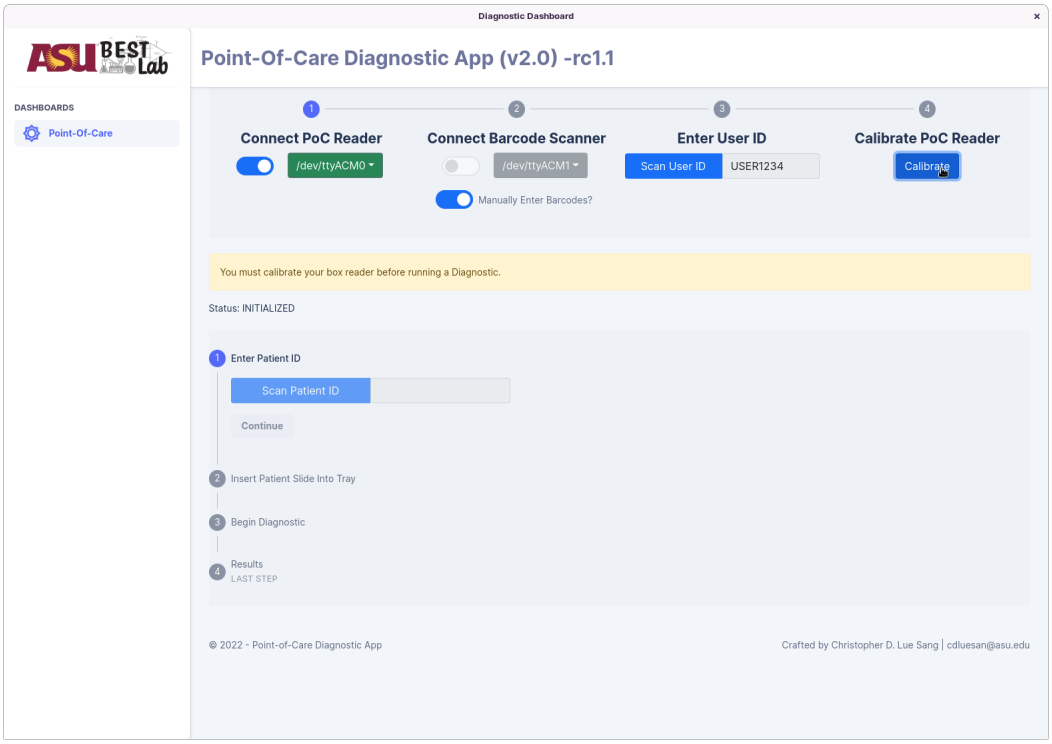

Figure 2.2: Screenshot of The POC Desktop Application

2.1 High Level Hardware Implementation (HW)

To better understand the contributions of this research a thorough understanding of the POC reader's hardware is required. The reader's electronics are composed of two commercially available off-the-shelf (OTS) breakout boards and two custom printed circuit boards (PCB). The OTS boards are the Arduino UNO (see Figure 2.4 D) and the TLC547 breakout board by adafruit.

The custom PCBs are designed to emit and capture light sent through the lateral flow assay (LFA) housed in the removable tray (see Figure 2.4 A,B,C). All boards are stacked onto each other starting with the Arduino UNO (see Figure 2.4, 2.5). The UNO contains the main microcontroller unit (MCU) which coordinates all actions of the reader. The MCU is the Atmega2560 by Atmel.

Figure 2.3: POC Reader Hardware with Open Tray

The physical construction of the POC Reader is designed to block out external light while shining an excitation light through one of the eight diagnostic sites available in the removable tray apparatus. The MCU communicates with the LED Driver (TLC5947) to apply a constant current through one of the single site's excitation LEDs. The LED emits a green light (520nm). That light passes through a filter to further narrow the wavelength of light before passing through the LFA. The LFA contains an analyte that's been engineered to fluoresce when excited by green light. The fluorescence's emission is that of orange light (605nm). The LFA's emitted light passes through another filter to further limit the original excitation light before hitting a photodiode.

The photodiode is connected to a capacitor integrating circuit. When the photodiode is excited current is allowed to flow and build up on a capacitor. The MCU repeatedly records the voltage of this capacitor over the duration of the diagnostic. A highly fluorescent LFA sample will cause the voltage to build up quickly over the charging capacitor. Conversely, a low or non fluorescing LFA sample will cause the capacitor's voltage to build up slowly. This voltage ramp is the distinguishing metric between a positive and negative detection of the analyte.

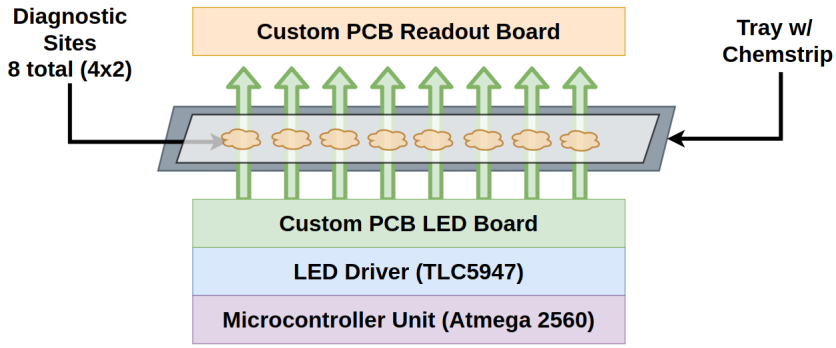

Figure 2.4: High Level Diagram of the POC Reader Hardware Components

Figure 2.5: Annotated Internal Component Assembly

2.2 Implementation Details of Firmware

The first bench-top implementation of this fluorescence hardware was developed by Obahiagbon et al. The process was manual. The excitation LED was controlled by a rocker switch and the output voltage was recorded on an oscilloscope. The operator was responsible for starting and stopping the test when the voltage ramp hit the rails the supply voltage. Thereafter a screen capture of the oscilloscope was saved and/or the voltage ramp was calculated and stored in a spreadsheet.

This manual method is not practical in a clinical setting. Not only does it produce slow results when processing many samples, it also places a huge burden on the

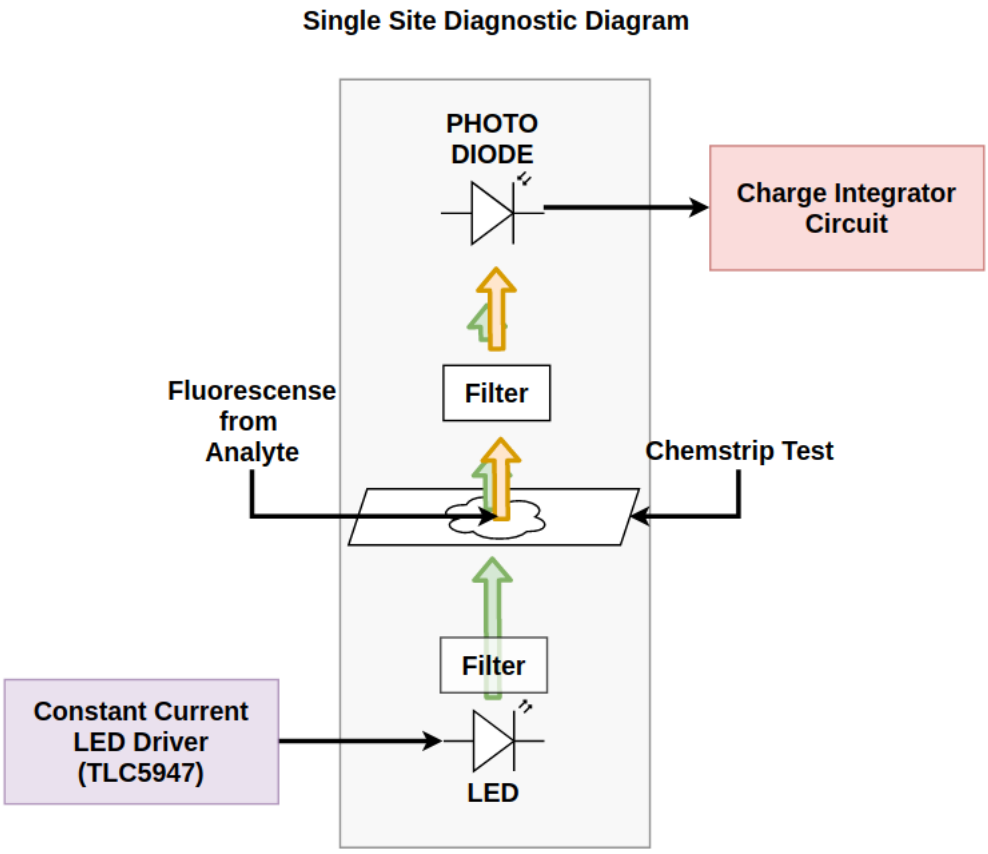

Figure 2.6: Single Site Diagnostic Diagram

operator to know the underlying technologies that make detection possible.

Hence, the multi-site fluorescent readers were created by Obahiagbon et al. leading to the latest design presented in this paper. From a high level the firmware starts with two main routines: setup and loop. The firmware was written using the Arduino framework with the Platform.io extension in visual studio.

2.3 The Arduino Framework

Arduino is a C/C++ language library made for embedded systems. The goal of this framework is to reduce the barrier to entry in writing embedded systems for common microcontroller vendors. The developers of Arduino accomplish this through

two main contributions. The first is the Arduino language. The language itself is just a library written in C/C++. Common routines such as: reading an analog value from an input/output (I/O) pin, and writing to an I/O pin are abstracted into a common interface (e.g. - analogRead(pin name)).

Typically different integrated circuit (IC) vendors would implement different methods for common MCU functions. These methods typically involve: setting device registers to particular values, reading device register values and setting up timers or interrupts. To save development time and reduce implementation errors, vendors often prepackage their own libraries into a standard development kit (SDK) and ship this along with their MCU ICs.

Similarly, the authors of Arduino develop libraries that when compiled implement the correct sequence of register setting and reading (and timer setting and reading) to accomplish a particular task for a specified MCU. The trade off is that these implementations may not be fully optimized for a particular MCU. The lack of 'optimization' can be apparent in excess clock cycles being used (e.g. - slower analog-to-digital (ADC) converter reads), or lack of configurability (e.g. - not using an available timer module that is free on the MCU).

This firmware presented in this work uses the Arduino framework but leverages some custom build parameters more easily configurable in Platform.io - an extension available in Microsoft's Visual Studio (VS) integrated development environment (IDE). Platform.io is an embedded systems development environment that allows the user to select different build systems (e.g. - Atmel, Espressif, Stm32, Arduino) for a variety of MCU boards. The firmware used in this work is available via a private git repository hosted on Github.com.

2.4 Top Level Firmware Routines

There are two top level routines that run on the POC reader firmware: setup and loop. Setup runs once on startup. Loop runs repeatedly. USB serial communication is essential for this application, therefore the loop function is not called until USB serial communication has started. While in the loop function, the USB serial buffer is checked for incoming messages. If messages are present, then they are parsed as JSON messages (see Figure 2.7).

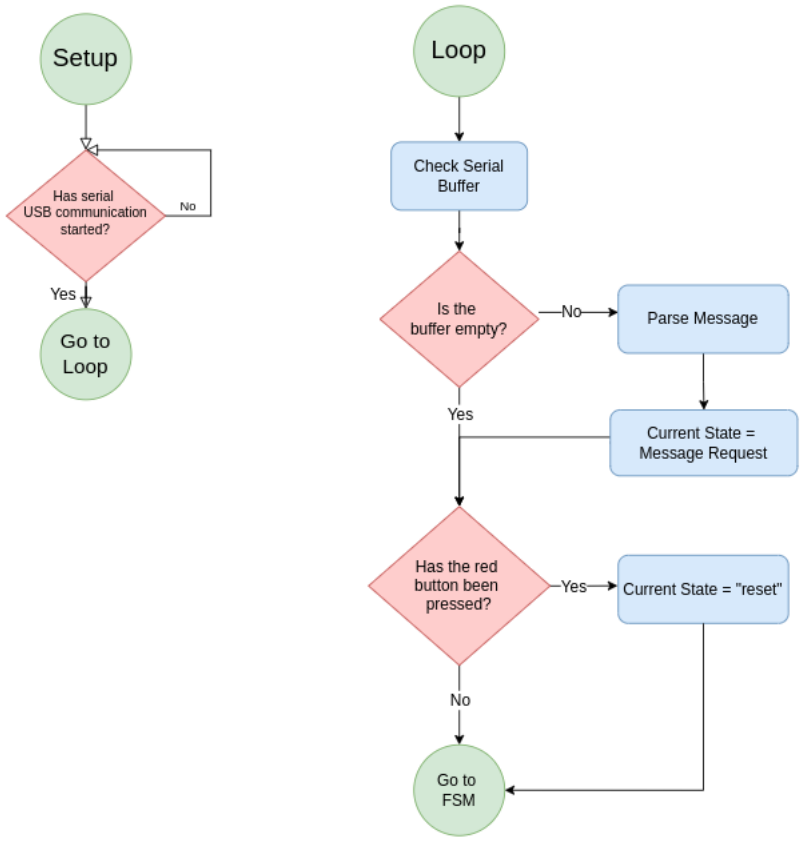

Figure 2.7: Setup and Loop Top-Level Routines

The JSON message format looks for two keys (sometimes referred to as data fields): 'req' and 'params'. The value of 'req' is a string of the subroutine to be

called/requested. The available subroutines are: boot, initialize, getMetaData, runDiagnostic, blink and reset. These subroutines are part of the overall finite state machine (FSM) that is called during the loop process (see Figure 2.8). If a request is called that doesn't match a subroutine's call name, an error response is provided as a syntax error. The syntax error specifies to the USB client that there was an issue parsing the requested message.

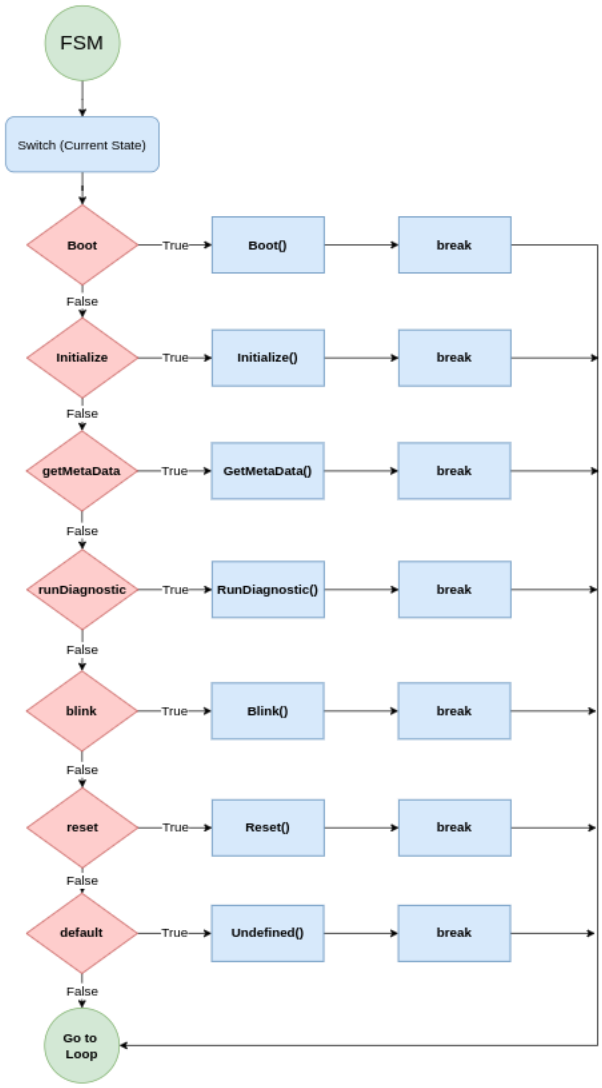

Figure 2.8: Main Finite State Machine (FSM) Routine

A thorough flowchart of each subroutine is provided in the appendix (see Figure

?). However, the most important subroutine is the run diagnostic process (called 'runDiagnostic') (see Figure 2.9). The 'runDiagnostic' request requires parameters to be passed that let the FSM know which diagnostic site to run and at what PWM value to run the diagnostic test.

There are some key aspects to the run diagnostic subroutine that should be noted. One, the routine is non-blocking. This means that the FSM continues to accept serial messages after printing out voltage and timestamps. This feature is important because it allows for the FSM to be reset if the diagnostic routine needs to be interrupted.

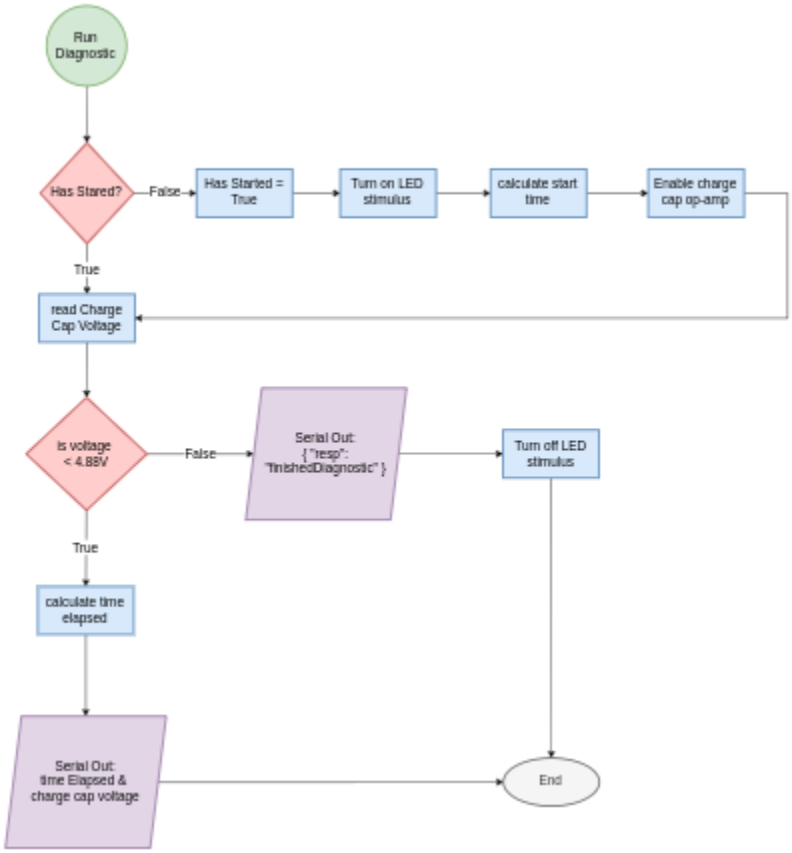

Figure 2.9: Run Diagnostic Routine

Two, the output of the diagnostic is not formatted as a JSON message. Instead the output is sent as two numbers delimited by a tab character and terminated by

a newline and carriage return character. This is to speed up the reporting of the diagnostic values. The client application is responsible for tracking when a diagnostic is initiated and ended, therefore knowing when and how to parse incoming serial messages from the POC reader.

2.5 High Level Software Implementation (SW)

The POC diagnostic desktop application is roughly composed of four layers of interfaces. The bottom most layer is the USB serial device controller which mediates USB serial connections on the host operating system. This interface is simple and is responsible for maintaining USB serial connections and sending and receiving serial communication messages.

Next, is the POC Driver layer which is responsible for parsing incoming responses and queuing outgoing requests. Lastly, the POC Controller is responsible for starting and stopping diagnostic requests, analyzing diagnostic data and ultimately mediating user interface (UI) requests with the POC Driver (see Figure 2.10).

The UI is made using node-webkit (NW.js). NW.js is a javascript framework for creating standalone desktop applications across multiple platforms: MacOS, Windows and Linux. Some key features of the UI allow for great flexibility by the operator without having to interact with the command line or raw serial output. These features are: connecting to a POC reader via USB, connecting a USB barcode scanner, scanning a user ID, conducting a calibration, scanning a patient ID, running a diagnostic and generating diagnostic data.

2.6 Clinical Usage Workflow

In collaboration with our clinical team at AIIMS a use-case workflow was established and developed in software. When the POC diagnostic application starts the

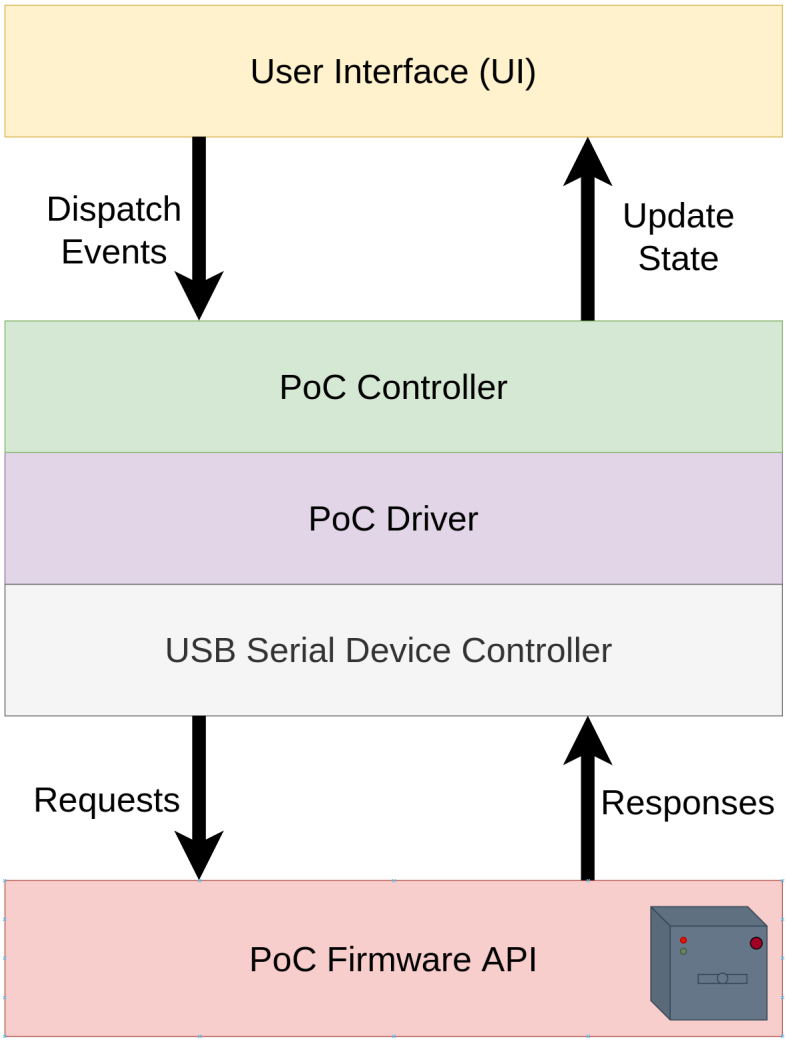

Figure 2.10: High Level Firmware and Software Interaction

user is greeted with a four step process before diagnostic runs can begin: 1) connect POC reader 2) connect barcode scanner, 3) enter user ID and 4) calibrate POC reader.

Once all four steps are complete the main diagnostic workflow is enabled. In the main diagnostic flow, the user does the following: 1) Enter Patient/Sample ID 2) Insert patient slide into tray and 3) begin diagnostic and 4) see results. When the results are presented the user has the option to copy the results and paste them into

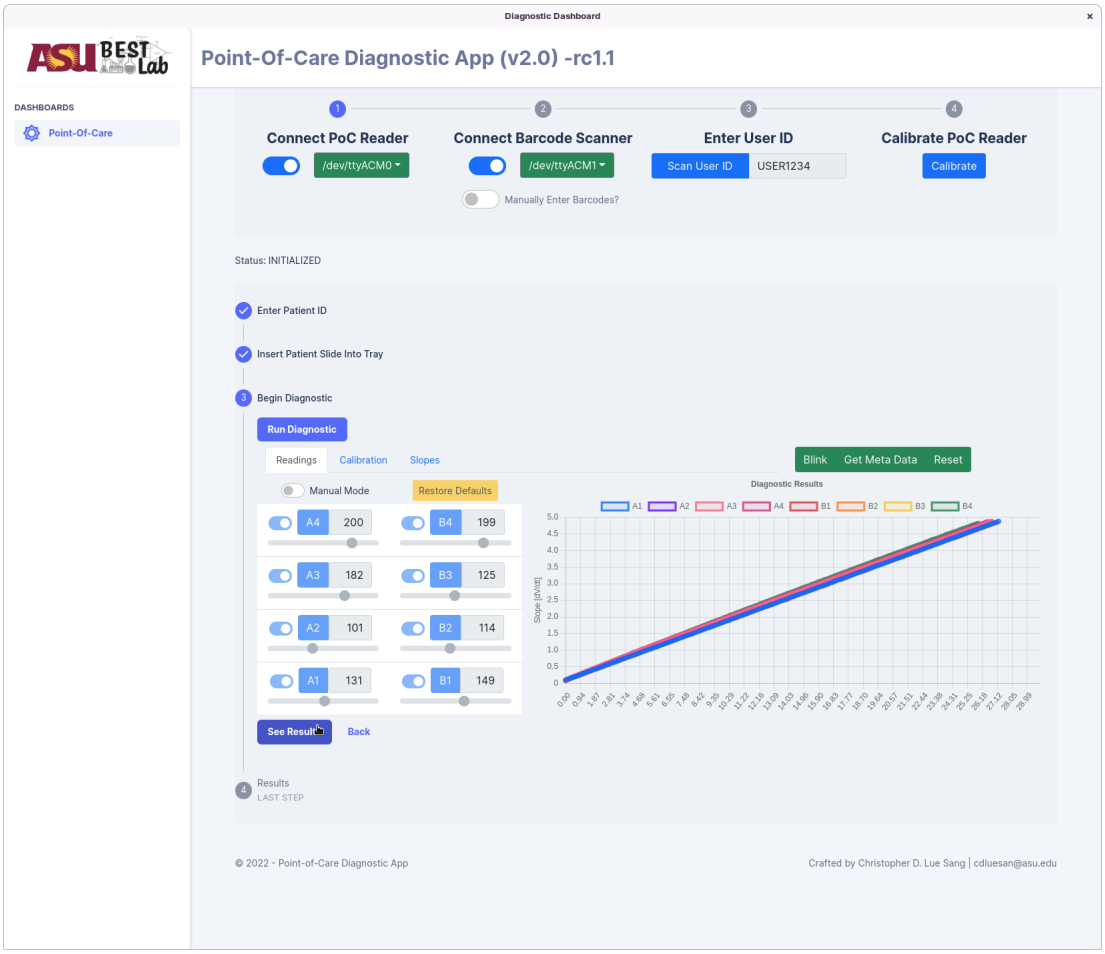

Figure 2.11: POC Desktop Application with Plotted Diagnostic Data

a spreadsheet (see Figure 2.11).

2.7 Calibration Routine

There are several broad categories of variation that are introduced into each diagnostic reading: environmental, mechanical and electrical. Mechanical variation comes from the variation of the physical components. The 3D printed enclosure produces variation in how the diagnostic sites are aligned between the light source and the light detector (photodiode). Additionally, the PCB components will also have slight variation in where the components are placed across different PCB assemblies. The

electrical components may have variation in their electrical characteristics (e.g. - bias current, impedance) even among components that should be the same part. But the magnitude of these variances should be within acceptable ranges. Ideally the mechanical and electrical variations are fixed per box and will only produce an offset in output readings when compared to one another.

Environmental variation however will change day-to-day and will produce a drift in the fluorescent readings if environmental conditions change. Therefore, to accommodate for these variations a calibration routine was devised to establish a baseline of behavior for each site. This routine is intended to be run once on application startup. Thereafter the clinicians or technicians can run through many diagnostic samples and their results are simply appended with the calibration results of that session.

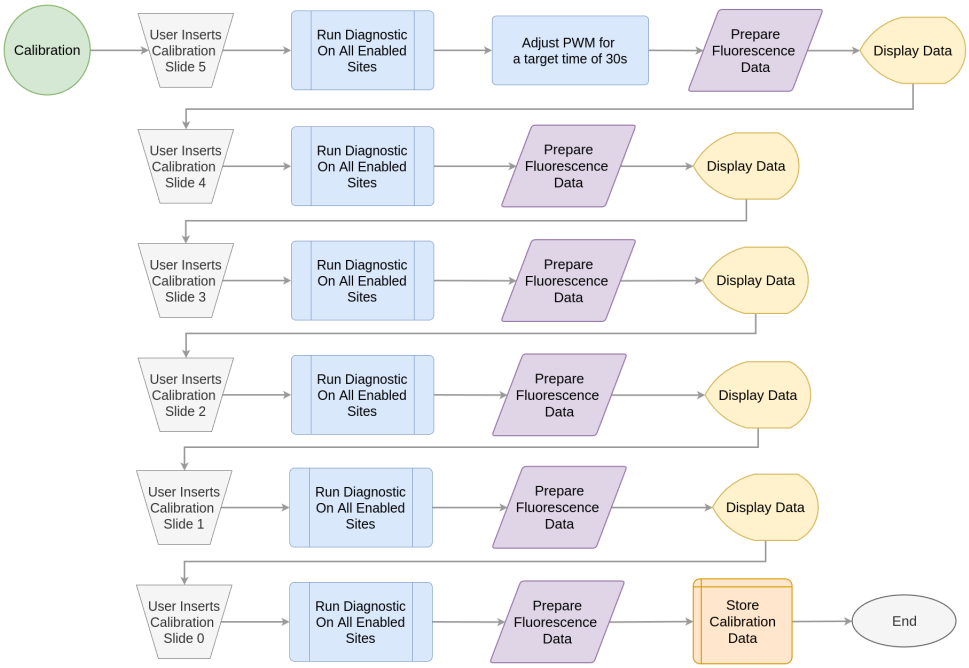

Figure 2.12: Calibration Flowchart

The calibration routine relies on providing the reader a phosphorus material that will produce a known amount of light emission given we provide it a known amount

of excitation light. Six slides were created by our lab to provide six different levels of known fluorescence. The phosphorus material is cut into sheets placed in dummy samples. Each calibration slide has neutral density (ND) filters layered on top of the phosphorescence sheet. The number of neutral density filters corresponds to the amount of fluorescence we want to expose to the reader. In short, slide 0 has no filters placed over its phosphorus sheet while slide 5 has five layers. Each layer reduces the fluorescence by half. This means that slide 5 emits $1/32^{\text{nd}}$ (or $1/2^5$) of the amount of light as slide 0.

Figure 2.13: Live Calibration Plots (Top) Slide 5 Completed Calibration Curves (Bottom) Slide 4 Incomplete Calibration Curves

During calibration the user is instructed to place a calibration side into the reader and then begin the calibration for that slide (see Figure 2.12). For slide 5, the PWM values of each diagnostic site is set to 255. The variation of each site manifests itself in different slopes. If a site is capturing less light than other sites it will take longer to complete a diagnostic, therefore its slope will be shallower. Conversely, if a site is integrating more quickly than other sites its slope will be steep. These slopes are derived from a linear fit of the diagnostic data (time elapsed and voltage data pairs). These slopes are used to calculate a new PWM value for each site that will produce the same integration time (aka linear slope) (see Figure 2.13 TOP) (see Equation 2.1).

$$\text{PWM}_{new} = \text{PWM}_{old} * \frac{\text{Calibration Slide 5 Integration Time}}{\text{Target Time (Typically 25s)}} \tag{2.1}$$

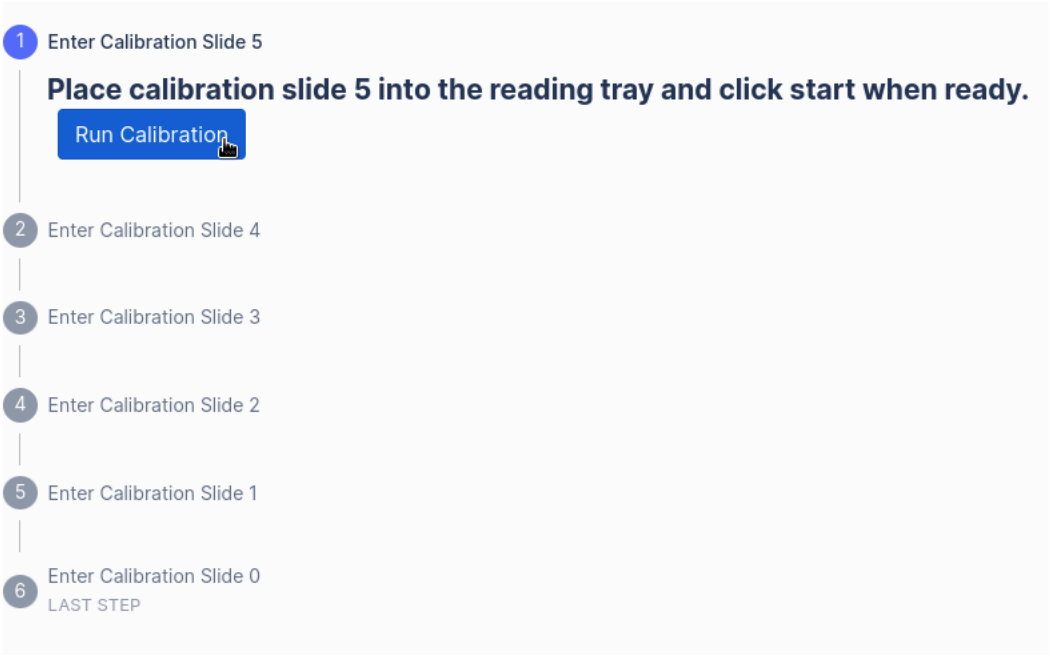

Figure 2.14: User Prompts to Perform Calibration

For slides 4 - 0, the linear slopes should be nearly the same. Meaning the user

should see overlapping diagnostic data for each site (see Figure 2.13 Bottom). Furthermore, as the slides go down in number and produce more fluorescence, the slopes of these overlapping lines should be steeper. At the end of the calibration routine the user can click on the 'calibration' tab and see the integration time for each site and for each calibration slide. The results should show an exponential curve corresponding to the exponential decrease in fluorescence (see Figure 2.15). A well performing calibrated POC reader will show closely clustered integration slopes for slides 4, 3, 2, 1 and 0.

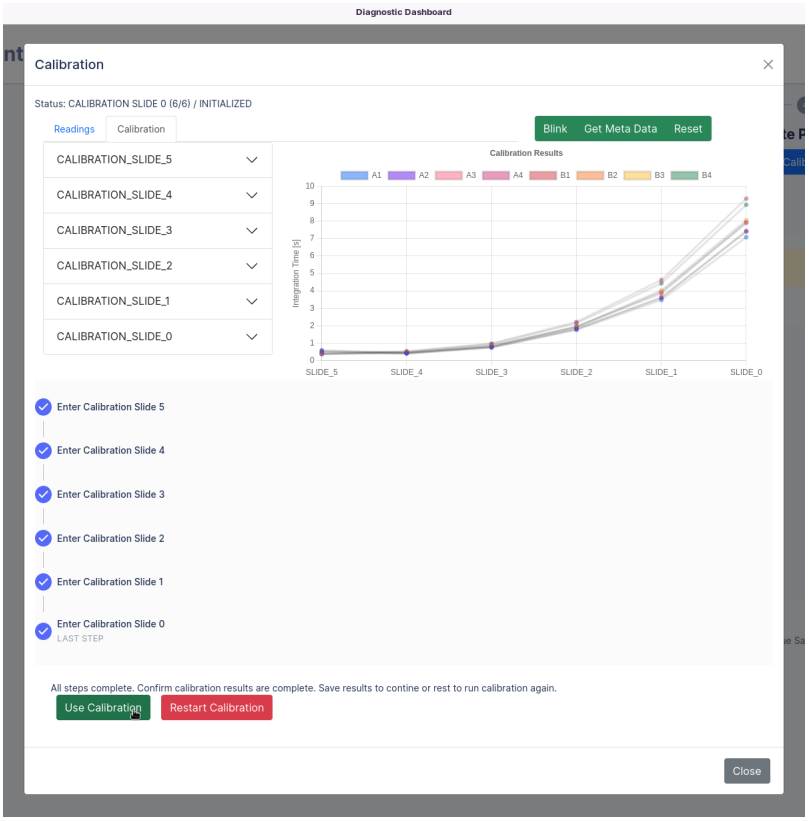

Figure 2.15: Screenshot of Calibration Curves

2.8 Running a Diagnostic

As part of the clinical workflow the user is prompted to scan a patient ID and insert the patient slide into the POC reader's tray before being allowed to run a diagnostic (see Figure 2.16). These simple checks help to ensure a reliable workflow when running hundreds or thousands of patient samples.

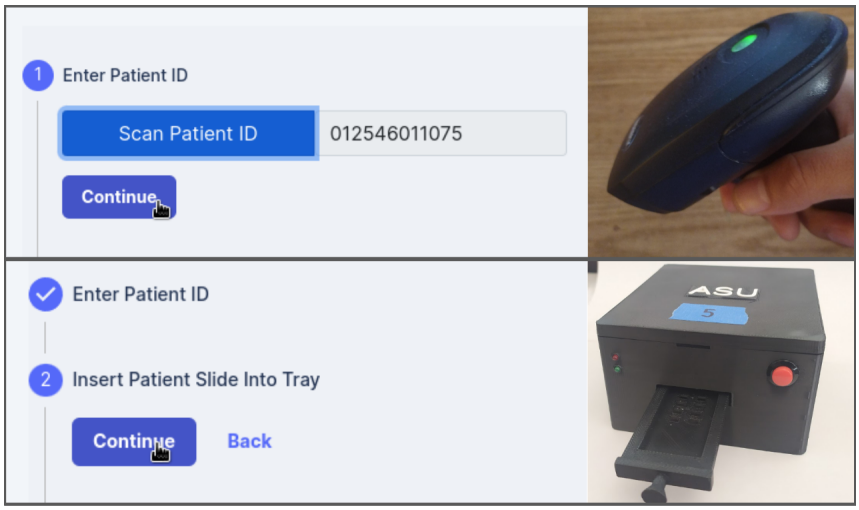

Figure 2.16: User Prompts and Pre-Diagnostic Steps

None of the firmware routines are blocking. This allows the firmware to receive requests while processing an ongoing request. When the diagnostic routine is called, the specified diagnostic site begins signal generation - the act of: enabling its LED output, recording voltage on the charge capacitor and reporting the voltage along with the time elapsed to the serial monitor.

The UI application initiates this signal generation with the run diagnostic request. The firmware reports: when it has started the request, the values the request generates and when the diagnostic has completed. The UI uses these states and data to update the interface and display a live graph to the user. The user has the ability to stop a diagnostic during the reading. This is useful for troubleshooting.

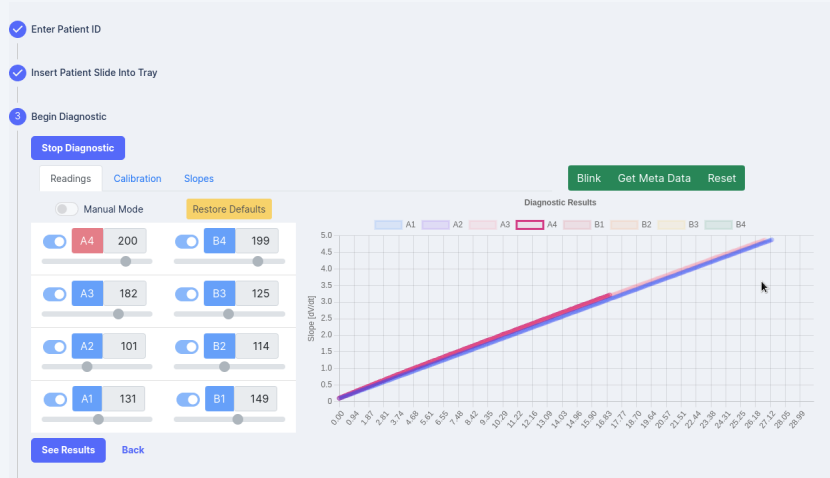

Figure 2.17: Screenshot of Live Diagnostic Data

2.9 Diagnostic Results

The output readings for a diagnostic are the change in voltage over the change in time (dv/dt). The data points are provided over serial in real-time. The integration slope is directly proportional to the fluorescence of the diagnostic site. A positive detection of an analyte on a given diagnostic site should show a steeper integration slope (i.e. - higher fluorescence). Ideally all eight diagnostic sites perform the same; meaning they produce the same integration slope given the same sample. This is essential in distinguishing between positive and negative results.

At the end of the diagnostic run the user is presented with a table featuring the key values extracted during the diagnostic routine (see Figure 2.18). The key values featured are the slope of the linear regression for each diagnostic site along with the linear fit's y-intercept, correlation coefficient and duration. Similarly, the results of the calibration routine are also presented. Each diagnostic site has an exponential fit applied to its fluorescence readings. The exponential fit's growth rate, and initial value are recorded along with the correlation coefficient and resulting PWM values.

Figure 2.18: Diagnostic Results Table

Chapter 3

EVALUATION

Environmental variation causes fluorescence readings to drift as the environmental conditions change. Exactly how that drift manifests in output readings is what our experimental setup will attempt to answer. The electrical components (e.g. - operational amplifiers, photodiodes, transistors) are temperature dependent. This means that they will have different electrical characteristics based on their temperature. Ideally, the POC reader will be operated in a temperature regime that is within the expected operating temperature of each component meaning their electrical characteristics should shift minimally and allow our calibration routine to account for this variation.

3.1 Experimental Setup

The device under test (DUT) is a POC reader. The reader is placed in a partially insulated environmental chamber. The chamber's temperature can be increased via an aluminum heated bed. The reader is placed on the bed but elevated 3mm off of the surface of the bed with a plastic shim. A suite of sensors are employed to provide readings from the environmental chamber. An ambient temperature and humidity sensor is elevated near the POC reader. And a temperature probe is taped to the POC reader's readout board through a hole in the lid of the reader's enclosure (see Figures 3.1, 3.2).

The sensors are connected to a raspberry pi 4 via the general purpose input/output (GPIO) pin bus. Their values are read via a python script that coordinates the sensing and logging of reader data over the course of the testing session. The chamber also

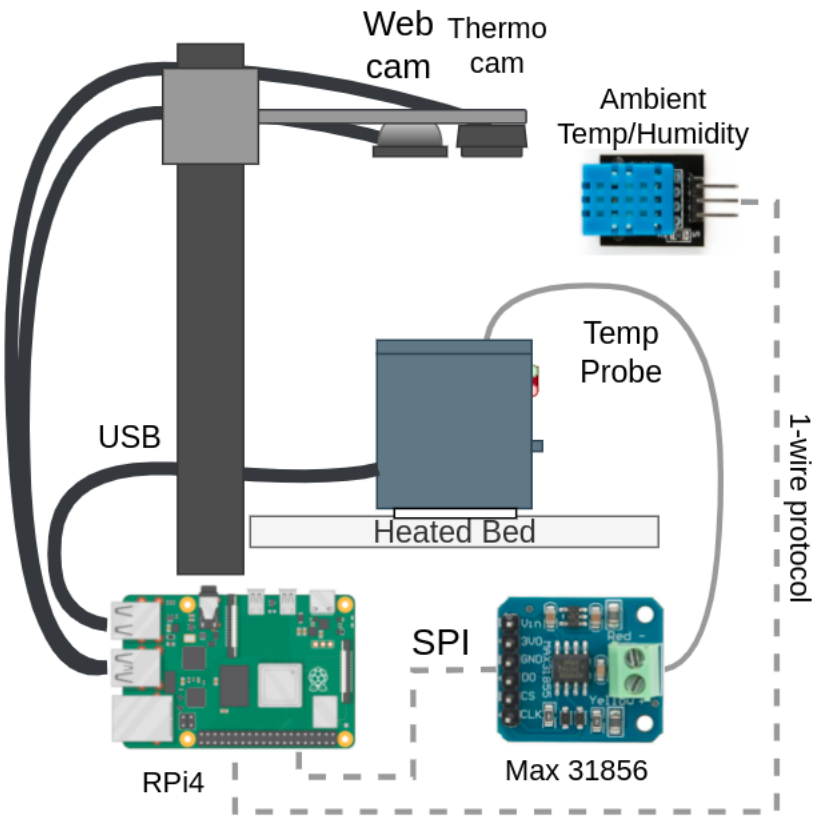

Figure 3.1: Thermal Test Chamber Components

contains a webcam and thermal camera which can provide spatial heating analysis of devices under test. The data presented in this work does not employ the thermal imaging data but may be employed in work outlined in future work.

The POC reader is also attached to the raspberry pi via USB. The raspberry pi interacts with the reader via the python data logging script created for this testing. The python script sends commands via USB to interact with the firmware API and is structured very similarly to the desktop application.

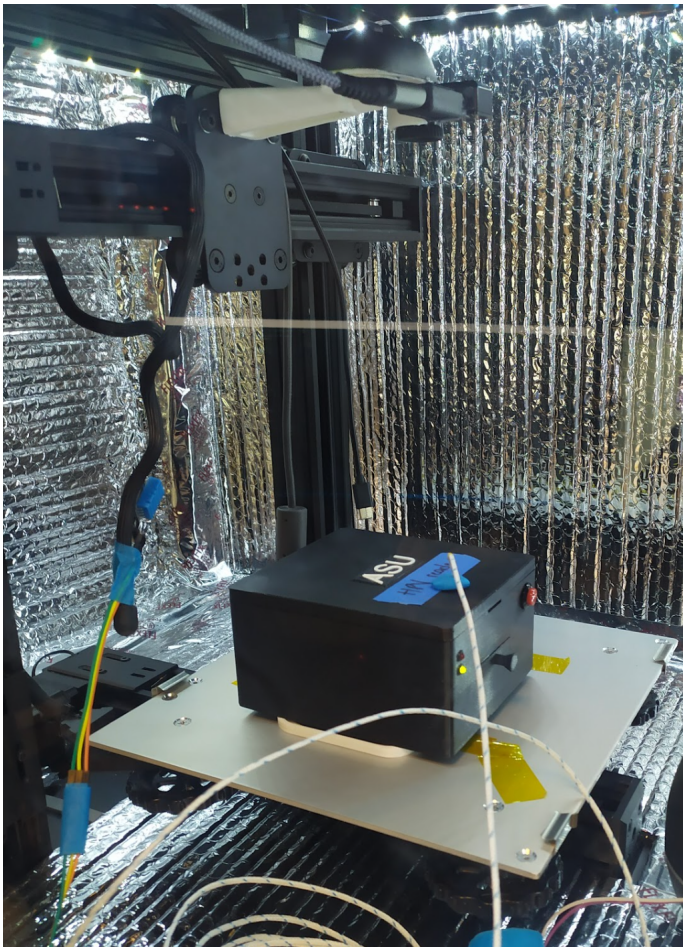

Figure 3.2: Image of Thermal Test Chamber with POC Reader

3.2 Data Collection

When the logging script is initiated the user is prompted via the terminal to run through a calibration routine. After the routine is complete a predetermined amount of test runs are initiated. The data presented in this work uses calibration slide 5 for the test runs. Slide 5 should present consistent diagnostic results over the duration of the test. If variation is observed, this means that environmental factors (or other sources of variation) are impacting the performance of the diagnostic sites.

The data is logged in two files: the session transcript, and the diagnostic results.

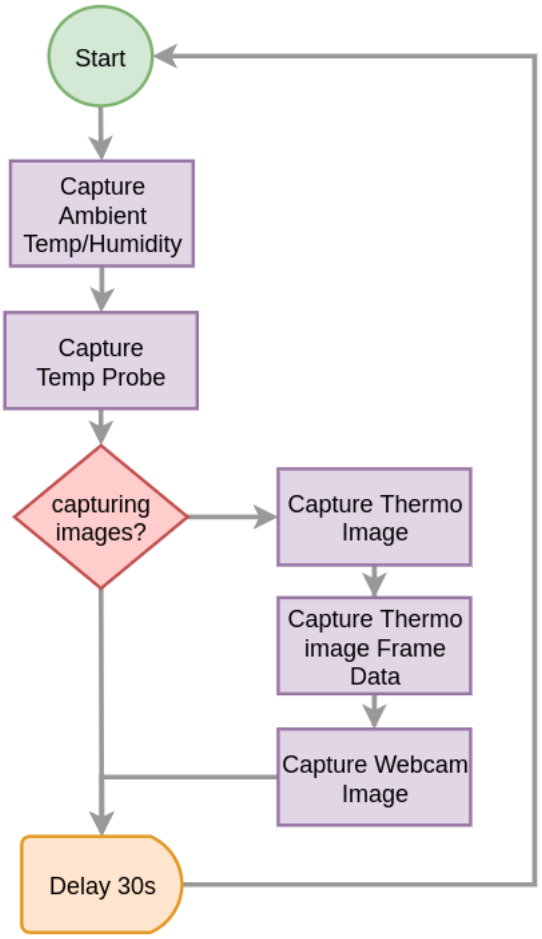

Figure 3.3: Thermal Test Chamber Data Collection Routine

The session transcript logs events supplied by the firmware API and the client application. The client application, in this case, is the python data logging script. Events are logged along with a timestamp and message. The message contains details about the logged event. Typically the events mimic the application state (e.g. - starting diagnostic, running diagnostic, running calibration, etc . . .). The diagnostic results are formatted in a comma separated values (csv) file. This file is easily viewable in a spreadsheet program. The columns (or 'fields') of data are: timestamp, diagnostic site, ambient temperature, ambient humidity, temperature probe, linear regression

data (i.e. - slope, correlation coefficient, intercept) and the duration of the test.

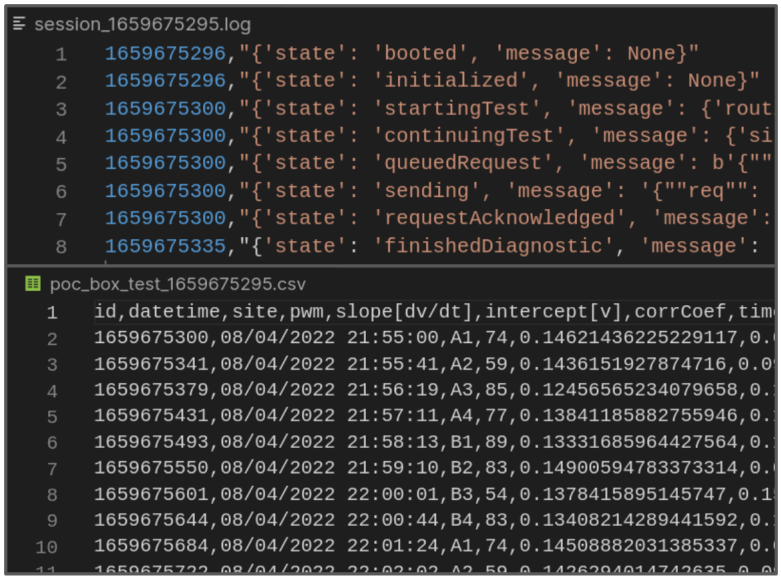

Figure 3.4: Screenshot of Diagnostic Results (Top) and Session Transcript (Bottom)

Two sets of tests were performed. The first attempts to simulate a nominal working temperature environment. The temperature was constant (approx. 27°C) and 9.5 hours of testing was performed using the same PWM values generated at the start of the test. The second test increased the temperature of the chamber to approximately 45°C and ran tests for approximately 6 hours using the same PWM values as from the first set tests. Thereafter the temperature was allowed to decrease to 35°C over the course of 3 hours.

Keeping the same PWM values throughout both tests allows us to observe the sensor drift that we can attribute to environmental changes. The relationship that drift has to the change in temperature will be helpful in evaluating the reliability of the fluorescence readings and the ability of the embedded system to detect faults or non-reliable readings.

Another source of errors comes from the USB serial communication. Sometimes, the USB communication between the client application and the POC firmware pro-

duces errors (i.e. - parsing errors). These errors were captured in the session log along with a timestamp. The frequency of these errors may correspond to temperature increases.

3.3 Results

Trials 1 and 2 used the same PWM calibration values. These values instruct the POC reader to drive the diagnostic site LEDs at a particular duty cycle. A greater PWM appears brighter, but more accurately leaves the LED on for a greater duration for a given unit of time. This ultimately has the effect of charging the readout capacitor more quickly, thereby creating a sharper integration slope and quicker integration. By keeping the calibrated PWM values the same between both trials we can observe the shift in performance as environmental factors change.

The calibration performed as expected. The integration slopes increased exponentially in line with the expected increase of fluorescence (see Figure 3.5). Ideally each site should have identical integration times (and integration slopes); but non-idealities (i.e. - noise, drift, quantization errors) exhibit themselves and produce variation between each site.

The variation between each site is captured in the standard deviation between the sites' integration slopes for a given calibration slide (see Figure 3.6). For instance, calibration slide 5 should have the highest variation between all the diagnostic sites. This is because slide 5 uses uncalibrated PWM values to drive the LED stimuli. The results of calibration slide 5 lead to new PWM values that are used for slides 4 - 5.

Therefore, the standard deviation for calibration slides 4 - 0 should be much smaller than calibration slide 5. Our results agree with this expectation. However, the standard deviation does increase as the calibration slides descend in value (see Figure 3.7). This is due to the increased fluorescence of the lower value calibration

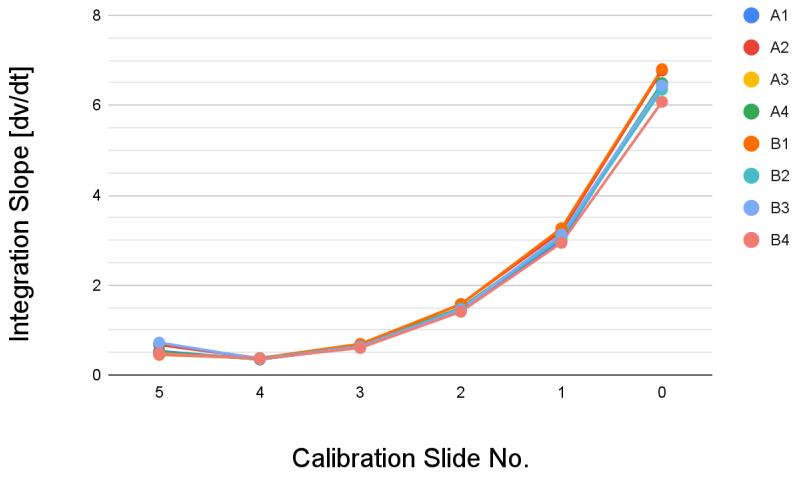

Figure 3.5: Environmental Chamber Calibration

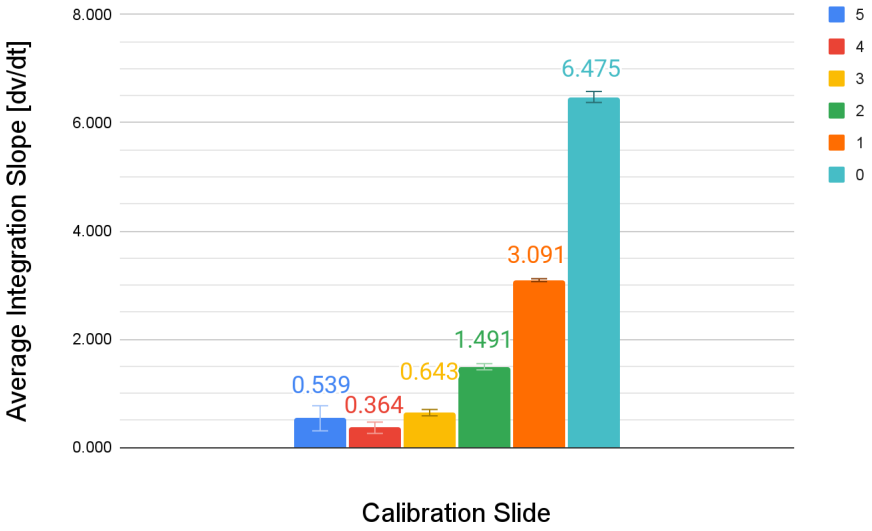

Figure 3.6: Average Integration Slope Per Calibration Slide (Before Trials)

slides. The analog to digital converter (ADC) has less time to sample the fast moving charge build up. The variation we observe on these quick integrations is likely due to quantization errors in the ADC.

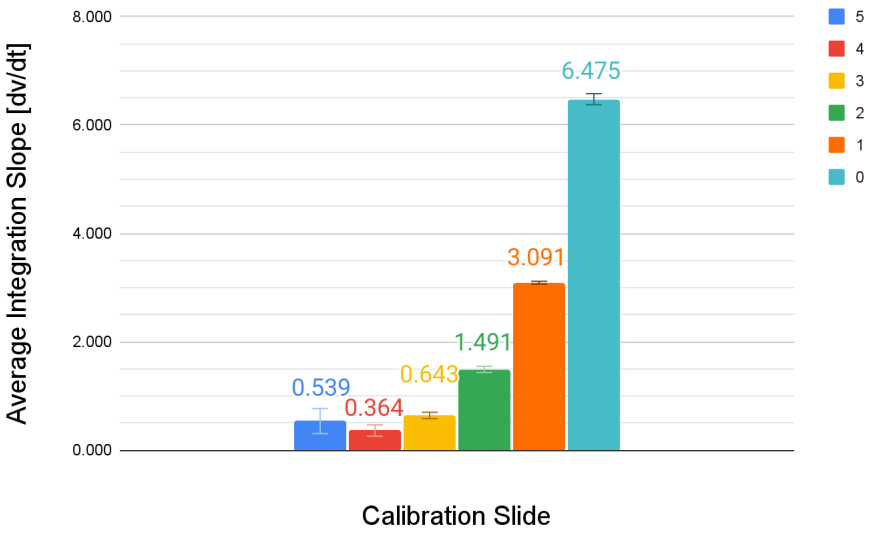

Figure 3.7: Standard Deviation per Calibration Slide (Before Trials)

3.4 Trial 1: Room Temperature Performance

The room temperature trial seeks to emulate a typical day of usage for the POC reader. The trial is composed of 100 runs per diagnostic site using calibration slide 5 as the test sample.

There is no obvious trend in sensor drift when operating at a nominal room temperature (29°C). The standard deviation of each diagnostic site is less than 1% of the magnitude of the integration slope. Under this behavior, a favorable signal to noise ratio (SNR) is expected with real world patient samples.

When correlated to the temperature probe, we see a weak relationship with the diagnostic sites' readings (see Figure 3.10). However we do see a link between diagnostic sites. This is acceptable, and somewhat expected, the diagnostic sites share electronic components and the temperature was kept constant so if there were a temperature dependence we would not see it in this trial.

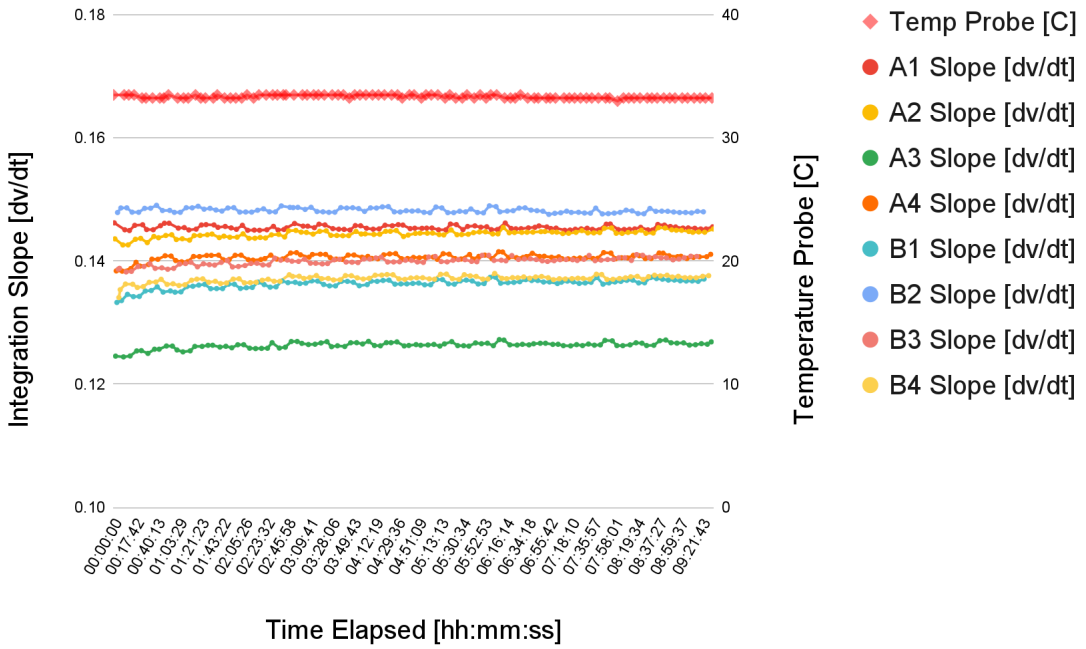

Figure 3.8: Trial 1: 100 Runs at Room Temperature

3.5 Trial 2: Heated Environment

For Trial 2, the environmental chamber was brought up in temperature until the temperature probe read 46°C. This temperature was chosen to represent a more extreme environment that the POC reader may experience in a triage environment. More extreme temperatures may be useful and may be explored in future work.

At about 6.5 hours into the trial the heated bed was turned off, and another 3 hours of testing was performed (see Figure 3.11). The integration slopes were clearly influenced by the environmental change. When correlated to temperature, the performance of each site can be seen to produce a positive or negative correlation with the temperature probe reading. The only exception to this influence appears to be site A1 (see Figure 3.12).

Site A1 maintained a steady performance throughout the trial as evidenced by its

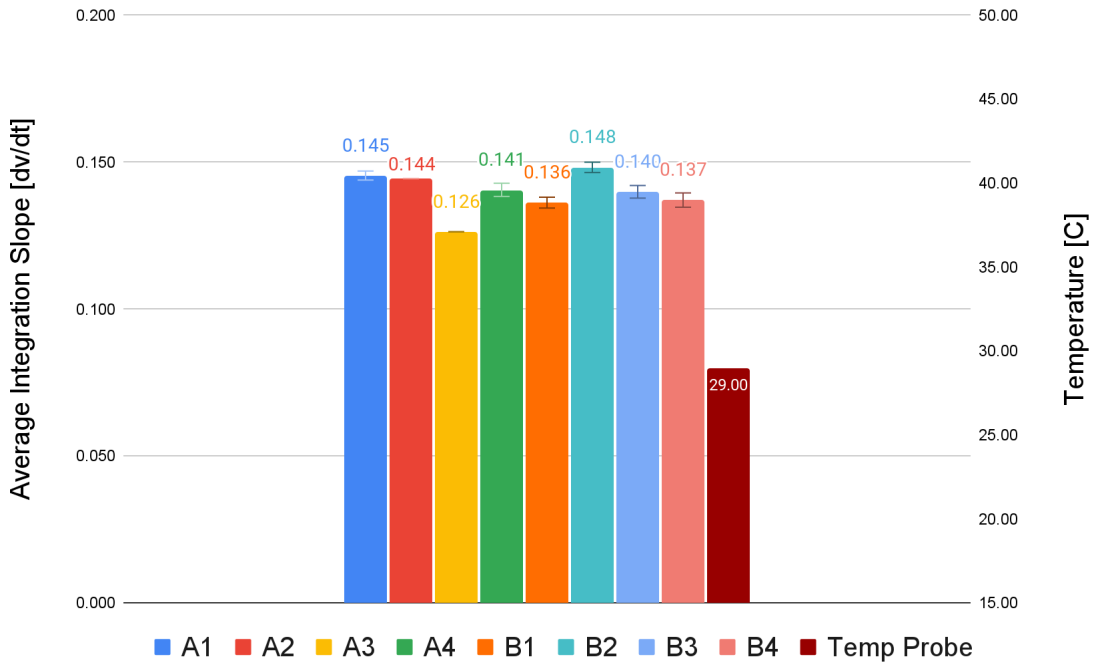

Figure 3.9: Average Integration Slope per Diagnostic Site

Temp Probe	1.00								
A1	0.05	1.00							
A2	-0.17	0.35	1.00						
A3	-0.07	0.29	0.89	1.00					
A4	-0.03	0.32	0.77	0.91	1.00				
B1	-0.17	0.08	0.86	0.91	0.84	1.00			
B2	0.31	0.48	0.03	0.16	0.31	0.03	1.00		
B3	-0.21	0.07	0.85	0.86	0.77	0.93	0.08	1.00	
B4	-0.04	0.04	0.74	0.85	0.81	0.91	0.13	0.91	1.00
	Temp Probe	**A1**	**A2**	**A3**	**A4**	**B1**	**B2**	**B3**	**B4**

Figure 3.10: Correlation Matrix of Trial 1 Runs

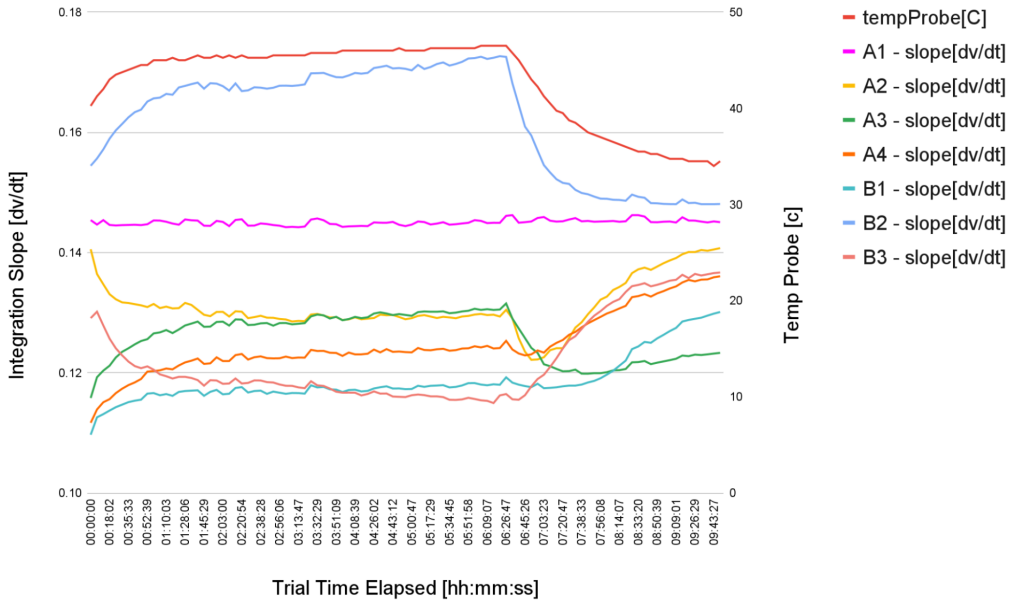

Figure 3.11: Trial 2 100 Runs in a Heated Environment

Temp Probe	1.00								
A1	-0.41	1.00							
A2	-0.66	0.19	1.00						
A3	0.83	-0.31	-0.41	1.00					
A4	-0.77	0.38	0.52	-0.30	1.00				
B1	-0.76	0.35	0.66	-0.28	0.95	1.00			
B2	0.97	-0.39	-0.54	0.93	-0.63	-0.61	1.00		
B3	-0.97	0.36	0.80	-0.81	0.69	0.72	-0.93	1.00	
B4	0.96	-0.41	-0.53	0.95	-0.58	-0.57	1.00	-0.92	1.00
	Temp Probe	**A1**	**A2**	**A3**	**A4**	**B1**	**B2**	**B3**	**B4**

Figure 3.12: Correlation Matrix of Trial 2 Runs

small standard deviation (less than 1%). The other sites' standard deviations varied between 3% to 8% of their median values throughout the trial. The POC reader's

internal temperature (provided by the temperature probe) on average deviated by as much as 10% from its mean (see Figure 3.13).

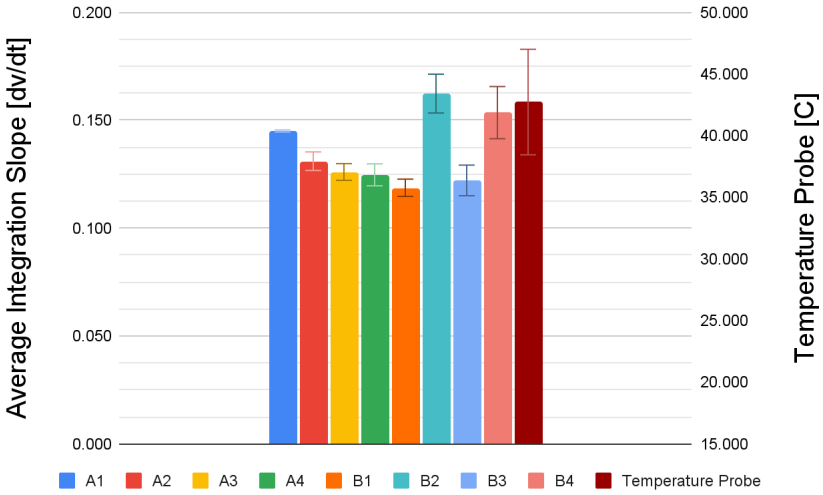

Figure 3.13: Trial 2: Average Integration Slope per Diagnostic Site

3.6 Post Heated Behavior

The POC reader exhibits some irreversible sensor drift after the heated trial. After undergoing a calibration routine the calibration curves for each diagnostic site exhibit greater spread than their pre-heated-trial calibration (see Figure 3.14).

Although the calibration process is intended to account for the variation between diagnostic sites by adjusting the PWM values, there seems to be limits to this approach. Ideally, each diagnostic site should give roughly the same integration slope for each calibration slide. But we observe large standard deviations for each calibration slide (see Figure 3.15). This means it will be more difficult to compare fluorescence results for a given sample taken at different diagnostic sites.

Nonetheless, between both trials the average integration slope for each site can be compared to each other. Site A1 and A3 depict the ideal behavior where their

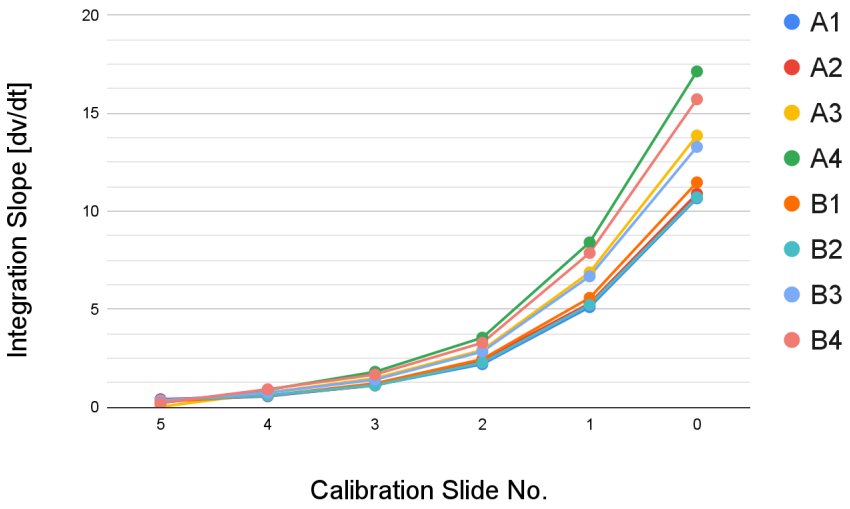

Figure 3.14: Post Heating Calibration Curves

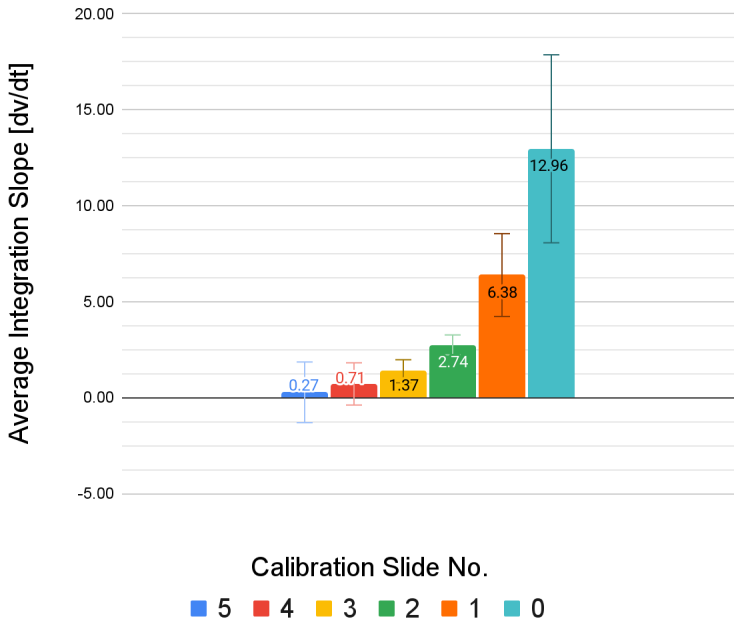

Figure 3.15: Post Heating Average Integration Slope per Calibration Slide

average slope in trial 1 is the same as in trial 2. All other sites exhibit a shift in the average slope across both trials. The magnitude of these shifts vary from 0% to 15%

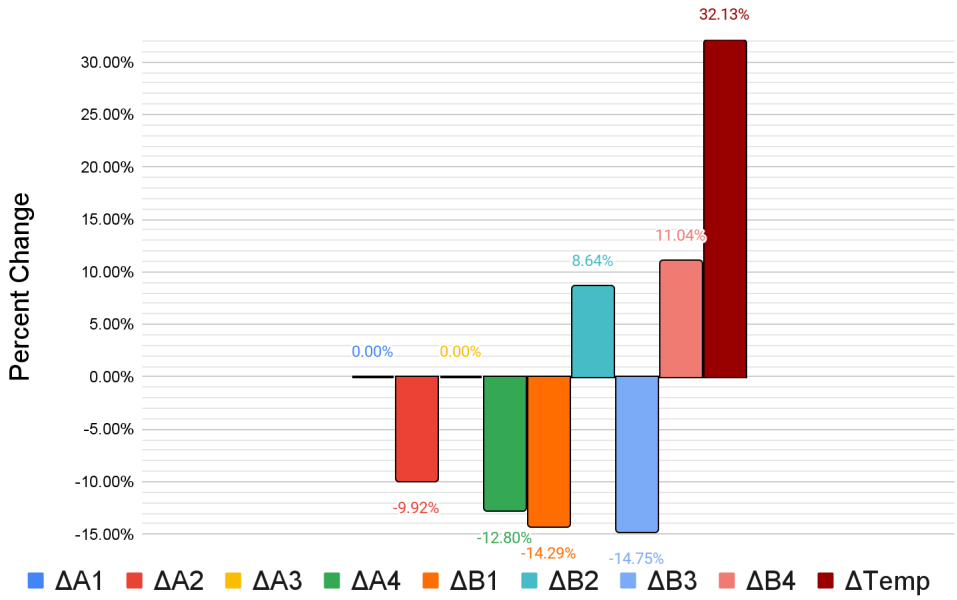

Figure 3.16: Percent Difference in Average Integration Slopes Between Trials

(see Figure 3.16). But more confounding is that the direction of the shift occurs in both directions. Some sites produce, on average, a higher fluorescence reading while other sites produce a lower reading.

The impact of these shifts will depend on the LFA design and the expected signal-to-noise ratio (SNR) of a positive detection versus a negative detection.

3.7 Fault Detection With Regression Analysis

Fluorescence readings provided by the POC reader are fit with a linear regression. In addition to the slope provided by this regression, the correlation coefficient and y-intercept are also calculated. The correlation coefficient for all diagnostic sites varied between 0.999 to 1.000 for both trials. This indicates that the diagnostic sites were responding linearly to the fluorescence emissions.

If the correlation coefficient for a particular linear fit were below 0.99, the diagnostic site is likely faulty or simply misaligned between the emission source and

emission capturing element. Although not experienced in these trials, field units have shown this behavior. The reader was suspected to have been damaged in shipping or damaged through prolonged usage. The diagnostic results provided by the desktop application includes the correlation coefficients for each diagnostic run. These values can be used to scrub the diagnostic data of bad readings.

Similarly, the calibration curves are fitted with an exponential regression. The fitted exponential curve parameters (i.e. - the starting value, the growth rate and the correlation coefficient) for each diagnostic site are saved along with the diagnostic results. This allows for each diagnostic site to be scrutinized at five different fluorescence levels. If the diagnostic sites are not responding exponentially as expected, we will observe poor correlation coefficients (less than 0.8). This information also helps throw out bad diagnostic data and identifies faulty hardware.

Both these approaches can be implemented in software or firmware. As this system is deployed with real patient samples the bounds of what acceptable readings look like will become more apparent and can be implemented in a fault detection algorithm.

3.8 Communication and Parsing Errors

As data is transmitted and received over USB, communication errors can arise in encoding and decoding messages from the transmitted byte arrays. Without any message integrity checks USB communication can be unreliable. To increase reliability an 'acknowledged' (ack) or 'not acknowledged' (nack) system was employed for the evaluation trials. In trial 1, 140 nacks were logged in the session transcript over 100 trial runs. When this occurs the request sent to the POC reader is repeated until an acknowledgement is sent back.

To generate an acknowledgement JSON messages (provided by the reader) are parsed and compared to the last JSON request provided. If the message failed to

parse or did not match the requested action, a 'nack' is generated and logged. Conversely, if the JSON message is successfully parsed and matches the last request, an acknowledgement is generated. This helps improve reliability over the USB communication channel.

Other methods of data reliability are available (e.g. parity bits, crc, checksums). They were not implemented in this hardware/software stack but may improve reliability of data transmission in future work. However, the results of the evaluation trials suggest that the system in place is capable of identifying bad data over long a duration of usage.

Chapter 4

CONCLUSIONS AND FUTURE WORK

Previous research by Obahiagbon et al. showed a promising low cost, POC, fluorescence based diagnostic system. The work presented in this paper improves upon that work by making the system more robust and usable in clinical settings. These contributions begin with an embedded system that exposes a reliable and simple API over USB serial. Next, this work introduces a client application that makes generating diagnostic data simple and auditable. Lastly, this work evaluates this system over two distinct 9 hour trials. The first of which represented a nominal usage environment and generated a standard deviation across all diagnostics sites of less than 1%. The second trial demonstrated the variation you may experience in heated environments where standard deviations of fluorescence integration slopes became as high as 15%. Finally, this work shows that hardware degradation can be captured in the regression analysis during the calibration process.

This work is in response to lab and field trials that used the POC reader to evaluate patient samples and encountered significant usability issues and significant variations in fluorescent readings (across different readers and different days of operation). The results of this work demonstrate an improved embedded system (and software application) that improves the reliability of the POC reader for portable health diagnostics.

4.1 Application Development Road-map

This system will be deployed with our clinical collaborators at AIIMS and Baylor University. The results from these future trials will refine our understanding of the

use case and the reliability of the system proposed in this paper. There are already several improvements intended to be integrated into the software application that will help bring further reliability to the POC reader.

1) Session Transcript Logging

Currently, session transcript logging is not implemented in the desktop application. The diagnostic results provided by the reader include key values that provide a top-level evaluation of a diagnostic. However, the session transcript (similar to that used for the evaluation trials) will help describe the performance of the POC reader hardware over time.

2) Diagnostic Results History

Currently it is up to the user to save diagnostic results in a separate spreadsheet. The current desktop application is intended to be a release candidate that features the essential features needed to generate diagnostic results. Persistent result history will alleviate the burden of maintaining a separate document with diagnostic data.

3) Remote Upload Of Diagnostic Data

Currently, the user is responsible for the diagnostic data generated by the desktop application. The current workflow has that user upload a spreadsheet containing diagnostic results into a database. Automatic remote upload would further alleviate the burden of the clinician processing patient samples and potentially allow for greater throughput of patient samples.

REFERENCES

Naseri, M., Z. M. Ziora, G. P. Simon and W. Batchelor, "Assured-compliant point-of-care diagnostics for the detection of human viral infections", Reviews in Medical Virology **32**, 2 (2022).

Obahiagbon, "Modeling, design, fabrication, and characterization of a highly sensitive fluorescence-based detection platform for point-of-care applications", (2018).

Obahiagbon, U., J. T. Smith, M. Zhu, B. A. Katchman, H. Arafa, K. S. Anderson and J. M. Blain Christen, "A compact, low-cost, quantitative and multiplexed fluorescence detection platform for point-of-care applications", Biosensors bioelectronics **117**, 153–160 (2018).

Serrano, B., M. Brotons, F. X. Bosch and L. Bruni, "Epidemiology and burden of hpv-related disease", Best practice research. Clinical obstetrics gynaecology **47**, 14–26 (2018).

Sohrabi, H., M. R. Majidi, M. Fakhraei, A. Jahanban-Esfahlan, M. Hejazi, F. Oroojalian, B. Baradaran, M. Tohidast, M. d. l. Guardia and A. Mokhtarzadeh, "Lateral flow assays (lfa) for detection of pathogenic bacteria: A small point-of-care platform for diagnosis of human infectious diseases", Talanta (Oxford) **243**, 123330–123330 (2022).

APPENDIX A

SUBROUTINE FLOW CHARTS

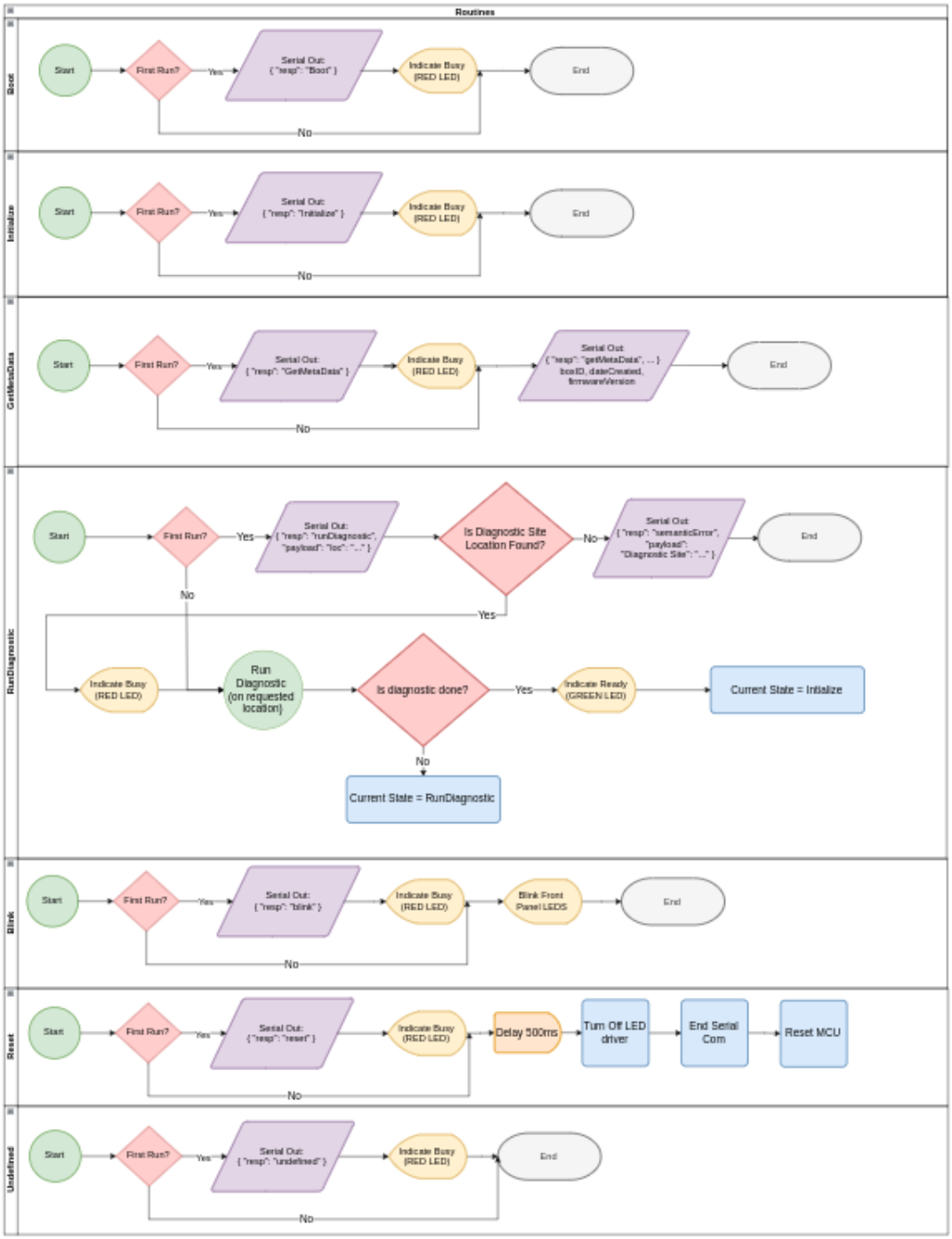

Figure A.1: Callable Subroutines Available in the POC Firmware API

BIOGRAPHICAL SKETCH

Christopher D. Lue Sang is a first generation American. His parents immigrated to the United States from the Caribbean (Jamaica and Trinidad). Prior to studying engineering he ran a small web design and development company in the Phoenix metropolitan area. His interest in software and web technologies led to a greater fascination with electronic hardware. After transferring to Arizona State he quickly became involved in university research. He was awarded two FURI grants during his undergraduate studies to investigate and prototype: a wearable breathing monitor and a soft actuator control system. During his senior year he joined the BioElectrical Systems and Technology (BEST) Laboratory where he contributed to the development of: portable gas sensors, underwater bycatch reduction devices and point-of-care health diagnostic systems. During his graduate studies, his interest in medical technology and business development led him to participate in Medtech Ventures as a program assistant where he helped to deliver course content on developing medical technology startups.